Am J Transl Res 2020;12(5):1600-1613
www.ajtr.org /ISSN:1943-8141/AJTR0105438

*Original Article*

# Comprehensive identification of a two-genesignature as a novel potential prognostic model for patients with medulloblastoma

Zihao Wang[1*], Xuesong Sun[2,3*], Lu Gao[1], Xiaopeng Guo[1], Chenzhe Feng[1], Wei Lian[1], Kan Deng[1], Bing Xing[1]

*[1]Department of Neurosurgery, Peking Union Medical College Hospital, Chinese Academy of Medical Sciences and Peking Union Medical College, Dongcheng District, Beijing, P. R. China; [2]Sun Yat-Sen University Cancer Center, State Key Laboratory of Oncology in South China, Collaborative Innovation Center for Cancer Medicine, Guangdong Key Laboratory of Nasopharyngeal Carcinoma Diagnosis and Therapy, Guangzhou, P. R. China; [3]Department of Nasopharyngeal Carcinoma, Sun Yat-Sen University Cancer Center, Guangzhou, P. R. China. [*]Equal contributors.*

Received November 25, 2019; Accepted May 8, 2020; Epub May 15, 2020; Published May 30, 2020

**Abstract:** Medulloblastoma is one of the most common malignant pediatric brain tumors and has a poor prognosis and high mortality. We investigated the prognostic significance of specific gene signatures and established a novel prognostic model for medulloblastoma patients. Ninety-seven differentially expressed genes between 69 medulloblastoma samples and 4 normal cerebellum samples were identified using the GSE68956 dataset. Univariate and multivariate Cox regression analyses revealed optimal prognosis-related genes, of which PFKP and STXBP1 exhibited significant prognostic values. A risk score model was then established to assess the prognostic value of the gene signature. Kaplan-Meier survival analysis demonstrated that patients with a high risk score had significantly poorer overall survival (OS, log-rank P = 0.003308). The concordance index (C-index) of the two-gene prognostic model for OS prediction was 0.752 (95% CI, 0.740-0.764). The area under the receiver operating characteristic curve (AUC) values for predicting 3-year and 5-year survival were 0.726 and 0.730, respectively. The risk score model was further validated in the ICGC cohort and PUMCH cohort using quantitative real-time polymerase chain reaction (qRT-PCR). Cox regression analyses were performed to assess the two-gene risk score model, metastasis stage, and chemotherapy as independent prognostic factors for medulloblastoma. The C-index of the comprehensive prognostic model composed of the two-gene signature integrated with clinicopathological features for predicting OS was 0.823 (95% CI, 0.739-0.907). The AUCs of the comprehensive prognostic model for predicting 3-year and 5-year survival were 0.774 and 0.759, respectively. Thus, the two-gene risk score model is a promising prognostic biomarker for medulloblastoma.

**Keywords:** Medulloblastoma, PFKP, STXBP1, prognostic model, bioinformatic analysis

## Introduction

Medulloblastoma is one of the most common malignant brain tumors in children, accounting for nearly 10% of all pediatric brain tumors [1-3]. It is commonly found in children aged 0-14 years and is slightly more common in males, with a male to female incidence rate ratio of 0.63 [3]. Surgery, radiotherapy and chemotherapy constitute a combined treatment for medulloblastoma [4]. However, medulloblastoma patients generally exhibit low survival rates and high mortality rates [3]. Therefore, assessments of prognostic and therapeutic factors are indispensable for the management of these patients.

Traditionally, medulloblastoma patients are stratified into average and high-risk groups according to clinical presentation, which helps to guide therapeutic decisions [5]. Nonetheless, clinical parameters show relatively limited and unreliable correlations with prognosis [6, 7]. To date, genome-wide expression profiling has identified molecular subgroups of medulloblastoma, including wingless (WNT), sonic hedgehog (SHH), group 3, and group 4 [8-10]. These four subgroups have distinct clinical and molecular

characteristics, contributing to the tumorigenesis and progression of medulloblastoma [11], yet the literature reports controversial and inconsistent prognostic significance for these molecular subgroups [5, 7, 10]. In general, the lack of precise prognostic biomarkers and models for survival assessment remains a major problem for improving the clinical outcomes of medulloblastoma patients.

In this study, we aimed to investigate the prognostic significance of specific gene signatures in medulloblastoma and to establish a novel promising prognostic model for medulloblastoma patients by performing a comprehensive gene expression profile assessment.

## Materials and methods

### *Data retrieval and processing*

Medulloblastoma expression profiles were downloaded from the Gene Expression Omnibus (GEO, http://www.ncbi.nlm.nih.gov/geo/) database, a public functional genomics data repository of high-throughput gene expression data, chips and microarrays [12]. After extensive data screening in GEO, the GSE68956 dataset was selected because it compares gene expression in 69 medulloblastoma samples and 4 normal cerebellum samples [13]. Moreover, both clinicopathological and survival data of the cohort were obtained for further analysis. Seven (10.1%) medulloblastoma samples were excluded because of a lack of clinical or survival data. In addition, level 3 RNA sequencing data and prognostic information for medulloblastoma patients were downloaded from the International Cancer Genome Consortium (ICGC, https://dcc.icgc.org/) database. The ICGC cohort, containing 60 medulloblastoma patients, was chosen as the validation set. All patients without prognostic information were excluded.

### *Identification of differentially expressed genes (DEGs)*

DEGs between medulloblastoma and normal cerebellum samples were identified using edgeR (https://bioconductor.org/packages/release/bioc/html/edgeR/) in R 3.5.1 [14]. Adjusted *P* values (adj. P) were applied to correct false positive results by using the default Benjamini-Hochberg false discovery rate method. Adj. P < 0.01 and |fold change (FC)| > 1 were considered the cutoff values for identifying DEGs [15]. A DEG hierarchical clustering heat map was constructed using the centered Pearson correlation method provided by the pheatmap package (https://cran.r-project.org/web/packages/pheatmap/) [16].

### *Construction and evaluation of the gene-based prognostic model*

Univariate Cox regression analysis was first performed on the DEGs to identify associations between the expression levels of genes and patients' overall survival (OS) using the survival package (http://bioconductor.org/packages/survival/) in R 3.5.1 [17]. Those genes with a *P* value < 0.05 identified by univariate Cox regression were further screened by multivariate Cox regression. Based on the Akaike information criterion (AIC), the optimal prognosis-related genes were determined to establish a prognostic risk score model for predicting OS [18]. Patients were divided into high- and low-expression groups according to the median expression levels of the prognosis-related genes [19]. Kaplan-Meier (K-M) survival curve analysis using the survival package was then performed to estimate associations between the expression levels of the prognosis-related genes and prognosis.

The prognostic risk score model was established with the following formula: risk score = expression level of $Gene_1$ × $\beta_1$ + expression level of $Gene_2$ × $\beta_2$ +...+ expression level of $Gene_n$ × $\beta_n$ [19, 20], where β represents the regression coefficient calculated by the multivariate Cox regression model. Subsequently, a prognostic risk score was generated for each patient. All medulloblastoma patients were divided into high-risk (high risk score) and low-risk (low risk score) groups according to the median value of their risk score [19, 20]. Next, a K-M survival curve was constructed to estimate the prognosis of patients with high or low risk scores, and survival differences between the high-risk and low-risk groups were assessed by a two-sided log-rank test. The prognostic performance was evaluated by the concordance index (C-index) and time-dependent receiver operating characteristic (ROC) curve analysis within 3 and 5 years to evaluate the predictive accuracy of the gene-based prognostic

model with the R package 'survcomp' (http://www.bioconductor.org/packages/survcomp/) and 'survivalROC' (https://cran.r-project.org/web/packages/survivalROC/) [21, 22]. Both the C-index and area under the curve (AUC) range from 0.5 to 1, with 1 indicating perfect discrimination and 0.5 indicating no discrimination. Next, 1000 bootstrap resamples were used to test the consistency between the predicted probabilities and actual survival outcomes. The performance of the gene-based risk score model constructed with the training set was similarly validated in the ICGC validation cohort.

Furthermore, univariate and multivariate Cox proportional hazards regression analyses were performed to evaluate the prognostic effect of various clinicopathological parameters and gene-based prognostic risk scores, especially to determine whether the gene signature is independent of other clinicopathological parameters. The prognostic performance within 3 and 5 years was assessed by the C-index and ROC curve analysis to evaluate the predictive accuracy of the comprehensive prognostic model composed of the gene signature and clinicopathological characteristics. All analyses were conducted using R version 3.5.1, and a *P* value < 0.05 was considered statistically significant. Hazard ratios (HRs) and 95% confidence intervals (CIs) are reported if necessary.

*Validation of prognosis-related genes using quantitative real-time polymerase chain reaction (qRT-PCR)*

A total of 28 fresh-frozen medulloblastoma and 28 paired normal specimens were obtained from Peking Union Medical College Hospital between January 2018 and September 2019. All procedures involving human participants were performed in accordance with the ethical standards of the Institutional Ethics Committee of Peking Union Medical College Hospital at the Chinese Academy of Medical Sciences & Peking Union Medical College and with the 1964 Declaration of Helsinki and its later amendments or comparable ethical standards. Informed consent was obtained from all participants included in the study. The primers used for qRT-PCR are shown in Supplementary Table 1. Total RNA was isolated from medulloblastoma tissues, and cDNA was synthesized from total RNA. The cDNA reverse transcription kit (TOYOBO, FSQ-101) was used to reverse transcribe RNA, and the SYBR Green PCR kit (Applied Biosystems, No. 4368708) was utilized to amplify the resulting cDNA. Detection was performed with a QuantStudio 5 Real-Time PCR System (Applied Biosystems; Thermo Fisher Scientific). Each experiment was conducted at least three times. The 2-ΔΔCt method was applied to calculate the expression level of genes relative to the housekeeping gene GAPDH.

*Functional and pathway enrichment analyses*

Coexpressed genes among the optimal prognosis-related genes were obtained from Coexpedia (http://www.coexpedia.org/), which is an online database of distinct context-associated gene coexpression networks inferred from individual series of microarray samples from several public depositories such as GEO and ArrayExpress [23]. Database for Annotation, Visualization and Integrated Discovery (DAVID, http://david.ncifcrf.gov/) is an online tool for gene functional classification, which provides an essential foundation for high-throughput gene analysis investigating the biological significance of genes [24]. DAVID was used for functional annotation and pathway enrichment analysis, including Gene Ontology (GO) enrichment and Kyoto Encyclopedia of Genes and Genomes (KEGG) pathway analysis, for the optimal prognosis-related genes and their coexpressed genes [25, 26]. A *P* value < 0.05 was considered statistically significant.

## Results

*Identification of DEGs*

Analysis of the GSE68956 dataset using edgeR revealed 97 DEGs, including 37 upregulated and 60 downregulated genes, between medulloblastoma and normal cerebellum samples (Supplementary Table 2). For visualization, the hierarchical clustering heat map of the DEGs is presented in **Figure 1**.

*Identification of prognosis-related genes*

By performing univariate Cox regression analysis on the 97 candidate genes in the cohort consisting of 62 medulloblastoma patients, we identified 5 prognosis-related genes, namely,

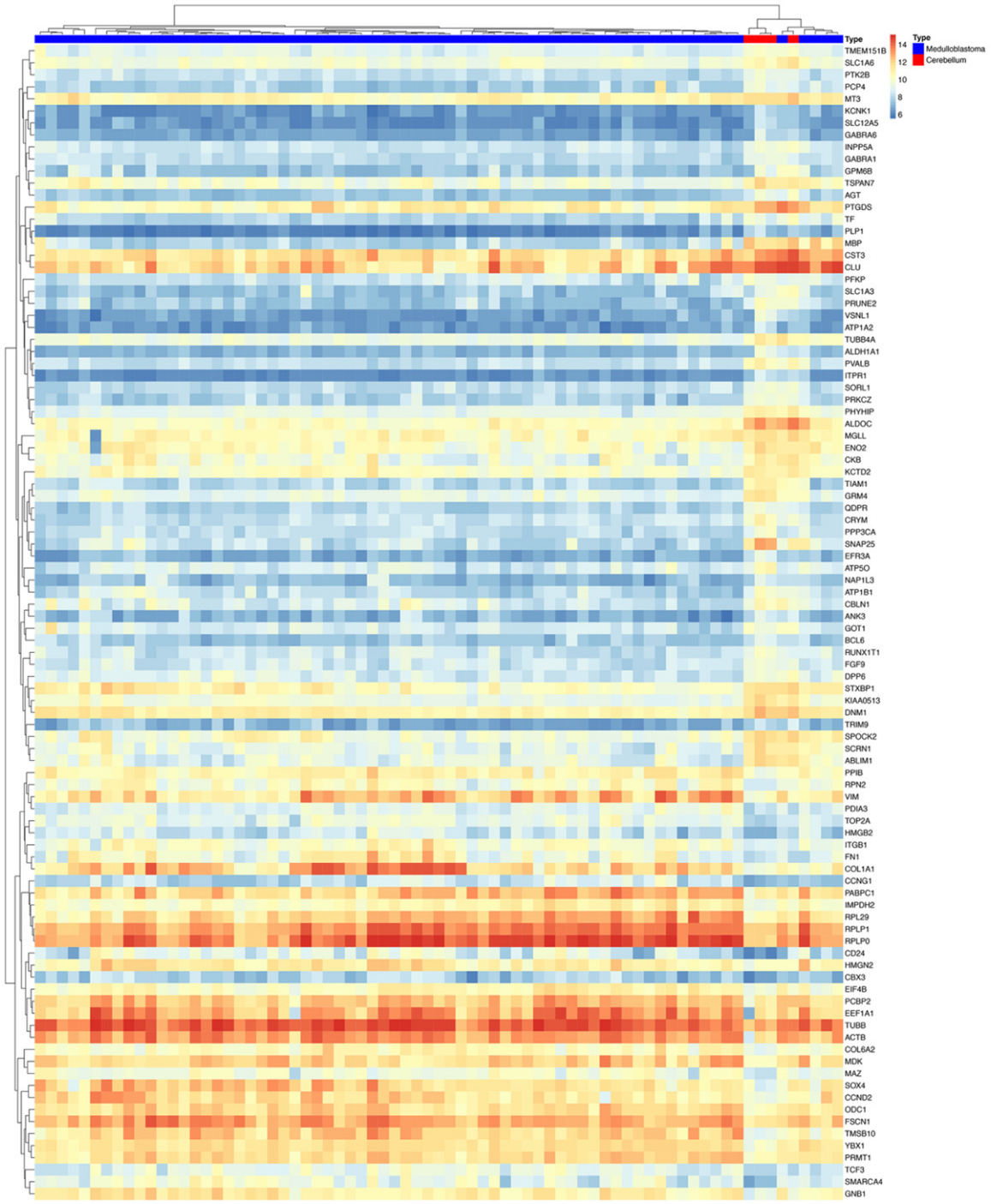


**Figure 1.** Hierarchical clustering heat map of differentially expressed genes between medulloblastoma samples and normal cerebellum samples. Red: upregulation; blue: downregulation.

RPL29 (HR 4.814), CCND2 (HR 0.198), IMPDH2 (HR 4.748), PFKP (HR 3.747) and STXBP1 (HR 0.470), which were indicated to have significant prognostic value ($P < 0.05$). According to multivariate Cox regression analysis, only two genes exhibited a significant prognostic value for medulloblastoma: PFKP (HR 4.875, $P = 0.037$) and STXBP1 (HR 0.109, $P = 0.043$). Expression of the above two genes between tumor and normal tissues was further validated in the GSE68956 dataset, which showed that both were significantly underexpressed in medullo-

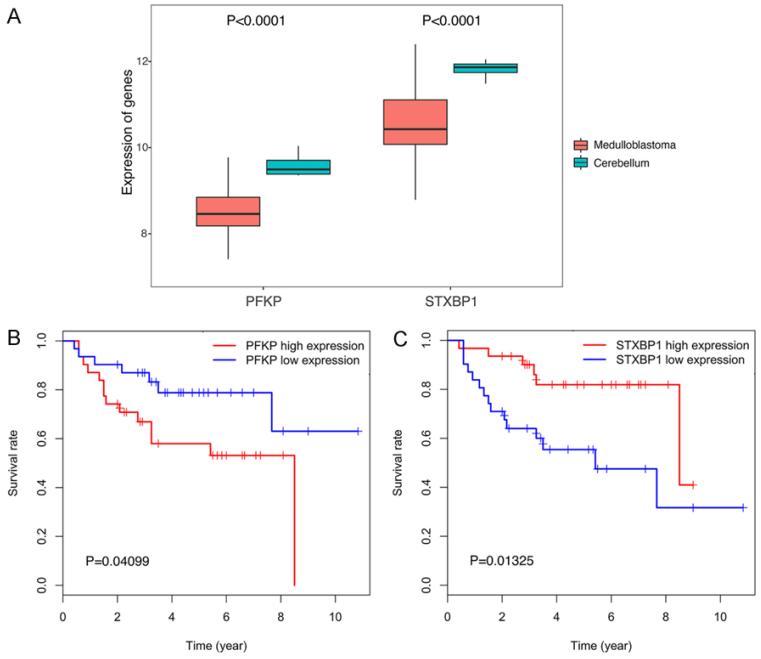


**Figure 2.** Expression and survival analysis of PFKP and STXBP1 in the GEO training cohort. A. Expression levels of PFKP and STXBP1 between the medulloblastoma group and the normal cerebellum group. B. The Kaplan-Meier survival curve indicated that the PFKP low-expression group had better OS rates than the PFKP high-expression group (log-rank P = 0.04099). C. The Kaplan-Meier survival curve indicated that the STXBP1 high-expression group had better OS rates than the STXBP1 low-expression group (log-rank P = 0.01325).

blastoma tissues (**Figure 2A**). In addition, K-M survival curves were constructed to assess associations between the expression levels of the prognosis-related genes and OS, and the results indicated a better prognosis for the PFKP low-expression group (log-rank P = 0.04099) and STXBP1 high-expression group (log-rank P = 0.01325) (**Figure 2B** and **2C**).

*Construction and evaluation of the prognostic model*

The prognostic risk score model was established with the following formula: risk score = expression level of PFKP × 5.42 + expression level of STXBP1 × -4.51. Subsequently, we calculated the prognostic risk score for each patient. All patients were divided into high-risk (high risk score) and low-risk (low risk score) groups based on the individual inflection point of the prognostic risk score (**Figure 3**). As illustrated in **Figure 4**, PFKP was significantly overexpressed and STXBP1 significantly underexpressed in the high-risk group compared with the low-risk group. In addition, K-M survival curve analysis demonstrated that patients with a high risk score had a significantly poorer OS than patients with a low risk score (log-rank P = 0.003308). The 3-year OS rates of the high-risk and low-risk groups were 64.5% and 89.6%, respectively, and the 5-year OS rates were 52.5% and 85.3%, respectively (**Figure 5A**). The C-index of the two-gene prognostic model for OS prediction was 0.752 (95% CI, 0.740 to 0.764; P < 0.001). Furthermore, the two-gene signature exhibited a favorable predictive ability for 3-year and 5-year OS rates, with AUC values of 0.726 and 0.730, respectively (**Figure 5B** and **5C**).

To confirm whether the prognostic signature has similar predictive value in different populations, we then used it to predict OS in an independent external validation cohort using the median risk score as the cutoff. As depicted in **Figure 3**, a total of 60 patients in the ICGC cohort were classified into low-risk (n = 30) and high-risk (n = 30) groups; the OS rate of the medulloblastoma patients in the high-risk group was significantly lower than that of those in the low-risk group (log-rank P = 0.021, **Figure 5D**). The two-gene signature constructed with the training set also displayed favorable predictive ability for the 3- and 5-year OS rates, with AUC values of 0.779 and 0.806, respectively, in the ICGC validation set (**Figure 5E** and **5F**).

In addition, we performed univariate and multivariate Cox regression analyses to evaluate the prognostic significance of the two-gene prognostic risk score together with various clinicopathological parameters, including age, sex, subtype, T stage, metastasis at diagnosis (M stage) and chemotherapy (**Table 1**). The univariate analysis indicated metastasis at diagnosis (M stage), chemotherapy and risk score to be significantly associated with OS in our cohort.

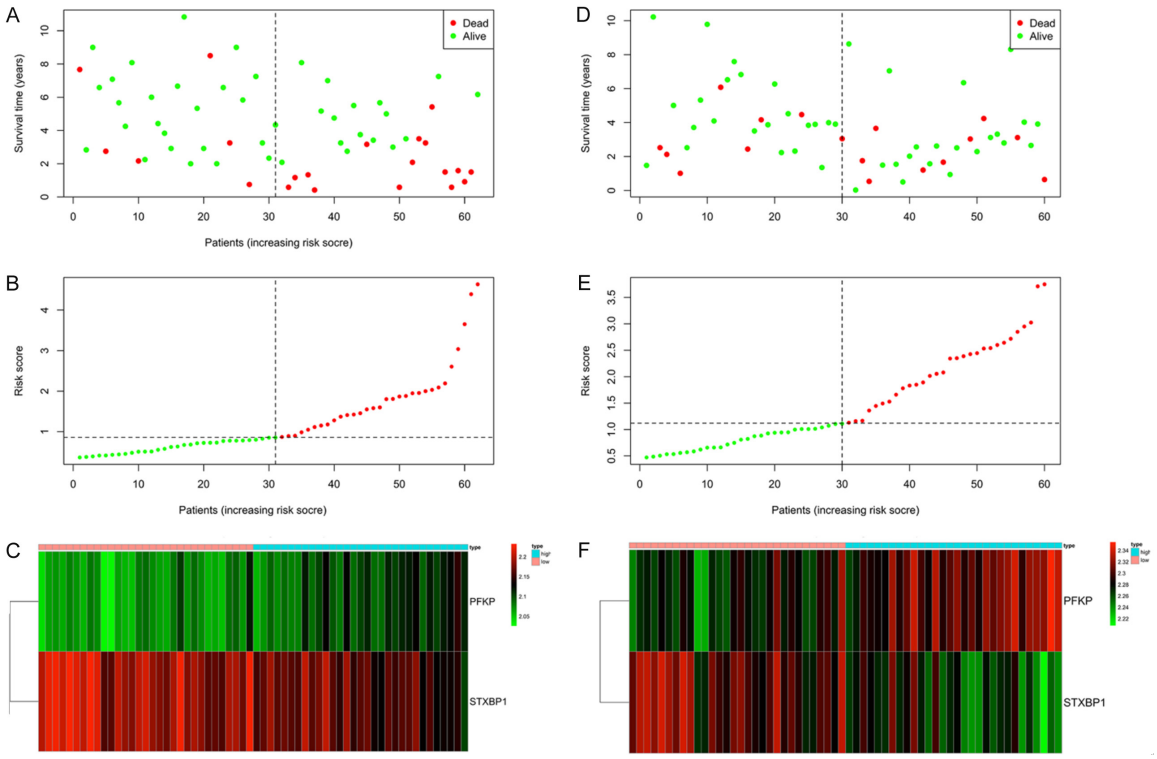


**Figure 3.** Risk score analysis of the two-gene signature of medulloblastoma in the training and validation cohorts. A, D. Patient survival status and time distributed by risk score. B, E. Risk score curve of the two-gene signature. C, F. Heatmap of PFKP and STXBP1 from the GSE68956 and ICGC cohorts. Colors from green to red indicate the expression level from low to high. The dotted line represents the individual inflection point of the risk score curve, by which the patients were categorized into low-risk and high-risk groups. Left panel: GSE68956; right panel: ICGC.

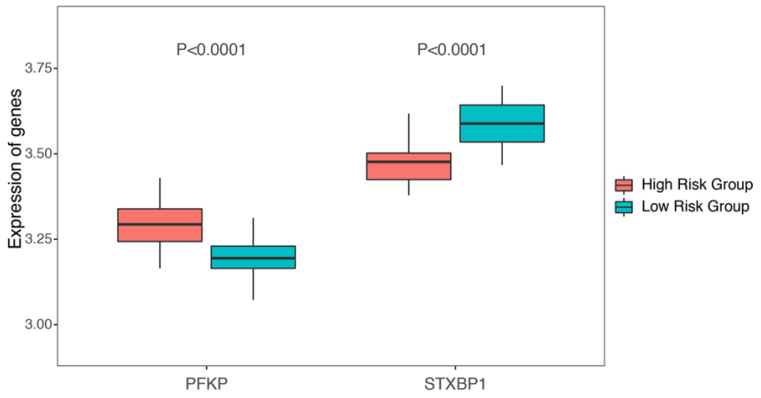


**Figure 4.** Expression levels of PFKP and STXBP1 in low- and high-risk groups.

However, other clinicopathological variables, such as age, sex, subtype, or T stage, were not significantly associated with prognosis. The K-M survival curves and log-rank test for all these clinicopathological variables are shown in Supplementary Figure 1. Multivariate analysis indicated that M stage, chemotherapy and risk score were significantly associated with OS, which demonstrated that the two-gene prognostic risk score can serve as an independent prognostic factor for medulloblastoma. The C-index of the comprehensive prognostic model, which is composed of the two-gene signature integrated with clinicopathological characteristics, for predicting OS was 0.823 (95% CI, 0.739 to 0.907; P = 0.001). The comprehensive prognostic model also showed a favorable predictive ability for 3-year and 5-year OS rates, with AUC values of 0.774 and 0.759, respectively (**Figure 6**).

*Validation of PFKP and STXBP1 using qRT-PCR*

As shown in **Figure 7**, the expression levels of PFKP and STXBP1 in 28 samples of medulloblastoma were significantly lower than those in

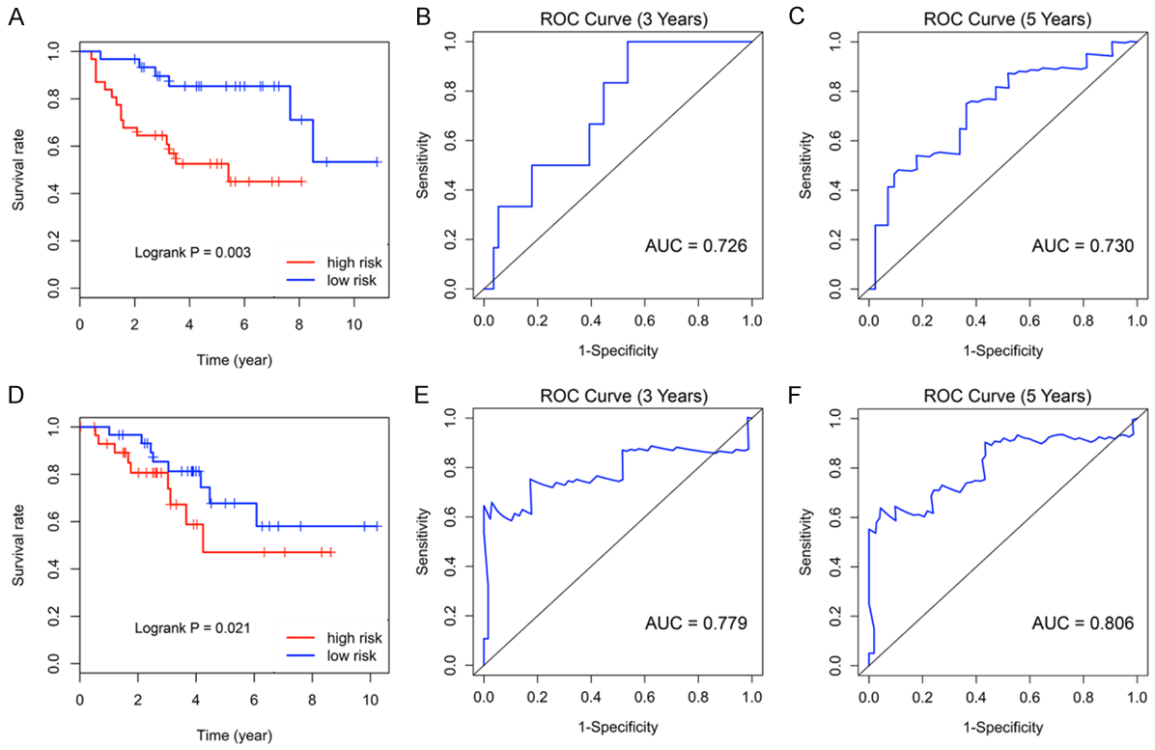


**Figure 5.** Kaplan-Meier survival curve analysis of the risk score for patient OS. A. In the GSE68956 cohort, the high-risk group had significantly poorer OS rates than the low-risk group (log-rank P = 0.003308). D. In the ICGC cohort, the high-risk group had significantly poorer OS rates than the low-risk group (log-rank P = 0.021). B, C. The prognostic performance of the two-gene signature demonstrated by the time-dependent ROC curve for predicting 3-year and 5-year OS rates in the GSE68956 cohort. E, F. The prognostic performance of the two-gene signature demonstrated by the time-dependent ROC curve for predicting 3-year and 5-year OS rates in the ICGC cohort.

**Table 1.** Univariate and multivariate Cox proportional hazards analyses of clinical parameters and risk score

| Variables | | No. of Patients | Univariate Analysis | | Multivariate analysis | |
|---|---|---|---|---|---|---|
| | | | HR (95% CI) | P | HR (95% CI) | P |
| Age | < 20 years | 23 | Reference | | Reference | |
| | ≥ 20 years | 39 | 1.392 (0.537-2.606) | 0.496 | 0.792 (0.248-2.526) | 0.694 |
| Sex | Female | 21 | Reference | | Reference | |
| | Male | 41 | 1.037 (0.417-2.584) | 0.937 | 1.290 (0.445-3.738) | 0.639 |
| Subtype | Classic | 48 | Reference | | Reference | |
| | Desmoplastic | 14 | 0.644 (0.187-2.221) | 0.486 | 0.395 (0.090-1.729) | 0.217 |
| T Stage | T1 | 3 | Reference | | Reference | |
| | T2 | 13 | 1.966 (0.207-2.640) | 0.556 | 0.497 (0.039-6.23) | 0.588 |
| | T3 | 27 | 1.561 (0.166-2.691) | 0.697 | 0.380 (0.030-4.804) | 0.455 |
| | T4 | 9 | 1.599 (0.122-2.090) | 0.720 | 0.594 (0.042-8.49) | 0.701 |
| | Tx | 10 | 5.768 (3.566-7.879) | 0.139 | 1.612 (0.133-5.592) | 0.708 |
| Metastasis at Diagnosis (M stage) | No (M0) | 43 | Reference | | Reference | |
| | Yes (M1-4) | 19 | 2.393 (0.995-5.754) | 0.0313 | 1.405 (0.489-3.734) | 0.048 |
| Chemotherapy | V, C, Cx | 36 | Reference | | Reference | |
| | V, C, Cx, VP | 16 | 2.013 (0.722-5.615) | 0.181 | 1.081 (0.317-3.684) | 0.901 |
| | Others | 10 | 2.432 (0.818-7.226) | 0.010 | 6.186 (1.555-14.609) | 0.009 |
| Risk Score | Low | 31 | Reference | | Reference | |
| | High | 31 | 4.185 (1.493-11.74) | 0.0065 | 7.128 (1.748-24.072) | 0.006 |

HR, hazard ratio; CI, confidence interval; Tx, T stage unknown; V, vincristine; C, carmustine; Cx, cisplatin; VP, etoposide; Others, V+C, or V+C+CC (cyclophosphamide), or V+C+VP.

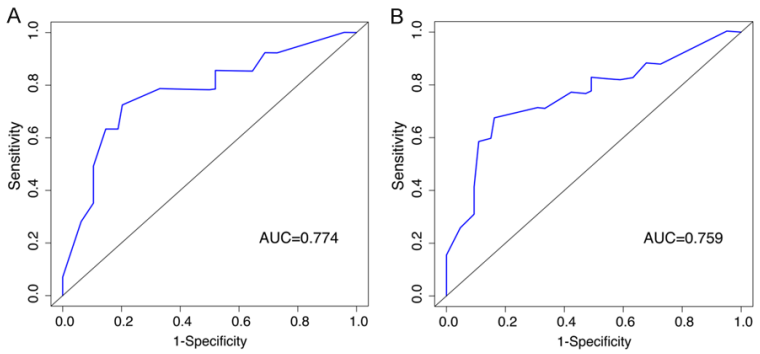


**Figure 6.** ROC curve analysis of the comprehensive prognostic model. A. The prognostic performance of the comprehensive prognostic model, composed of the two-gene signature integrated with clinicopathological characteristics, demonstrated by the ROC curve for predicting the 3-year OS rate (AUC = 0.774). B. The prognostic performance of the comprehensive prognostic model, composed of the two-gene signature integrated with clinicopathological characteristics, demonstrated by the ROC curve for predicting the 5-year OS rate (AUC = 0.759).

normal tissues; thus, the qRT-PCR results were consistent with the high-throughput sequencing data obtained from the GEO training cohort. K-M survival analyses also demonstrated a better prognosis for the PFKP low-expression group (log-rank P = 0.0263) and STXBP1 high-expression group (log-rank P = 0.03378). Finally, to investigate whether the prognostic risk score model can be applied to the PUMCH cohort consisting of 28 medulloblastoma patients, we calculated the risk score for each patient and used the median risk score as the cutoff. The 28 patients in the PUMCH cohort were classified into a low-risk group (n = 14) and a high-risk group (n = 14), and the OS rate of the medulloblastoma patients in the latter was significantly lower than that of those in the former (log-rank P = 0.002, **Figure 8A**). The prognostic two-gene signature also exhibited robust predictive ability for 3- and 5-year OS rates, with AUC values of 0.918 and 0.731, respectively, in the PUMCH cohort (**Figure 8B** and **8C**). These findings strongly support the reliability of our prognostic risk score model for predicting the prognosis of medulloblastoma patients, which might assist both physicians and patients with individualized survival predictions and facilitate better treatment decision-making and follow-up scheduling.

*Functional and pathway enrichment analyses*

A total of 257 genes coexpressed with PFKP and 292 genes coexpressed with STXBP1 were obtained using Coexpedia (Supplementary Table 3). GO enrichment analysis, including biological process (BP), cellular component (CC) and molecular function (MF) categories, was performed on PFKP and STXBP1 and their coexpressed genes; 77 of the genes are associated with BPs, 37 with CCs, 24 with MFs, and 35 with KEGG pathways (Supplementary Table 4). According to GO functional annotation analysis, genes in the BP category were significantly enriched in positive regulation of I-kappaB kinase/NF-kappaB signaling and glycolytic process (**Figure 9A**); CC category genes were significantly enriched in extracellular exosomes and the cytoplasm (**Figure 9B**), and MF category genes were significantly enriched in ATP binding and calcium ion binding (**Figure 9C**). In addition, KEGG pathway analysis mainly revealed enrichment in metabolic pathways, the biosynthesis of antibiotics, endocytosis and the HIF-1 signaling pathway (**Figure 9D**).

## Discussion

As reported in the literature, medulloblastoma is a complicated disease entity that can be stratified into different subgroups according to clinical, histopathological and molecular features [1-4, 8-10]. A few studies have investigated associations between the above methods of classification and prognosis of medulloblastoma patients to guide therapeutic decisions. However, most of these studies have reported controversial and inconsistent prognostic significance [5-7].

Zeltzer et al. [6] reported that the metastasis stage, adjuvant treatment, and residual tumor were clinical factors associated with prognosis in medulloblastoma. Based on the study of Ray et al. [27], the presence of metastatic disease at presentation is one of the strongest predictors of survival. Patients with desmoplastic or extensive nodular tumors are believed to have better survival, even after a reduction in therapy [28]. Pietsch et al. [7] also identified M stage as the only clinical factor associated with sur-

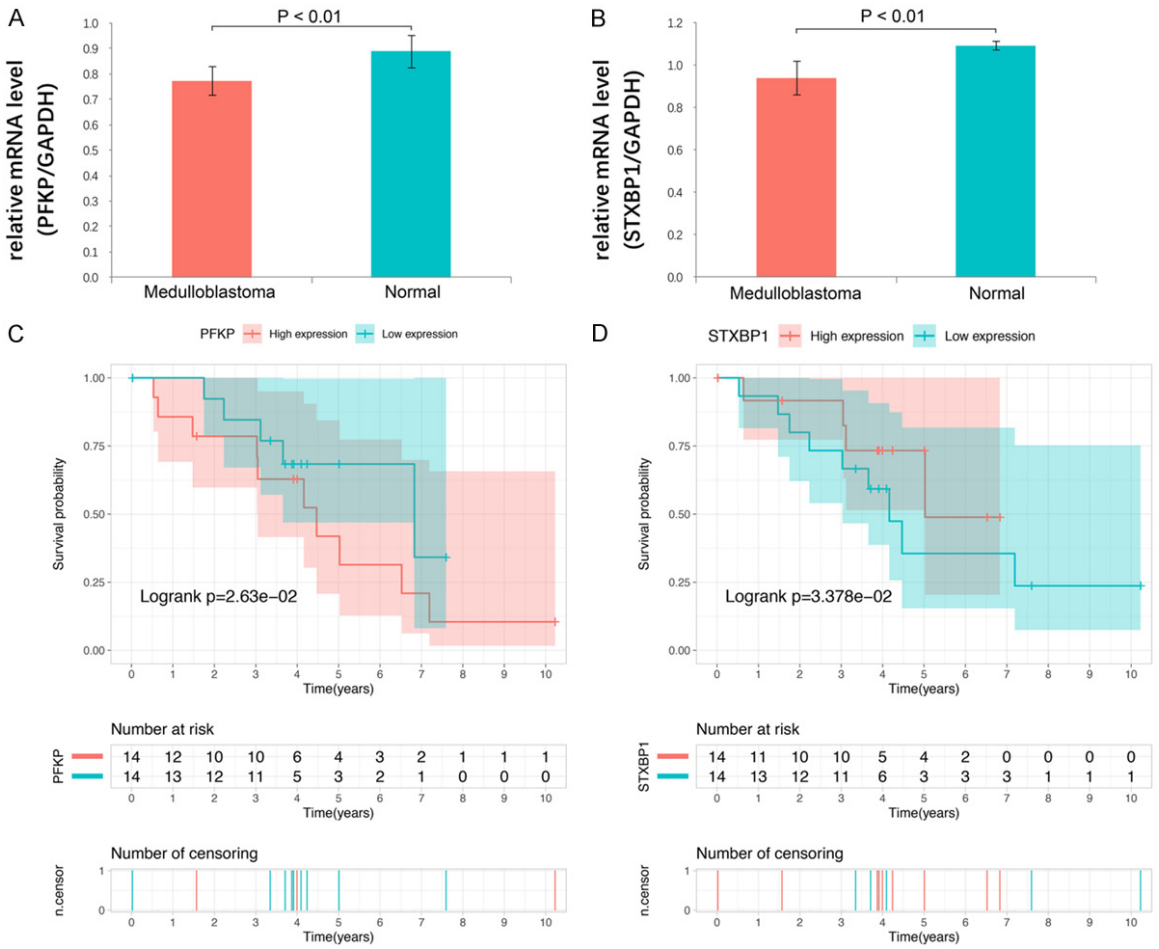


**Figure 7.** Expression and survival analysis of PFKP and STXBP1 using qRT-PCR in the training cohort. Relative expression levels of PFKP (A) and STXBP1 (B) between medulloblastoma and normal tissues based on qRT-PCR. (C) The Kaplan-Meier survival curve indicated that the PFKP low-expression group had better OS rates than the PFKP high-expression group (log-rank P = 0.0263). (D) The Kaplan-Meier survival curve indicated that the STXBP1 high-expression group had better OS rates than the STXBP1 low-expression group (log-rank P = 0.03378).

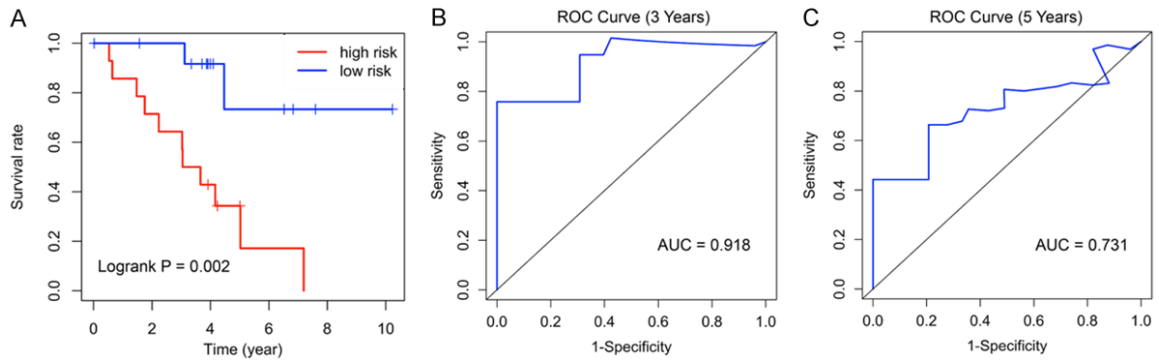


**Figure 8.** Survival analysis of the risk score for patient OS in the training cohort. A. Kaplan-Meier survival curves indicated that the high-risk group had significantly poorer OS rates than the low-risk group (log-rank P = 0.002). B, C. The prognostic performance of the two-gene signature demonstrated by the time-dependent ROC curve for predicting 3-year and 5-year OS rates in the training cohort.

vival. In our study, we found metastasis at diagnosis (M stage) to be an independent prognostic factor for medulloblastoma, consistent with previous studies. Furthermore, several studies

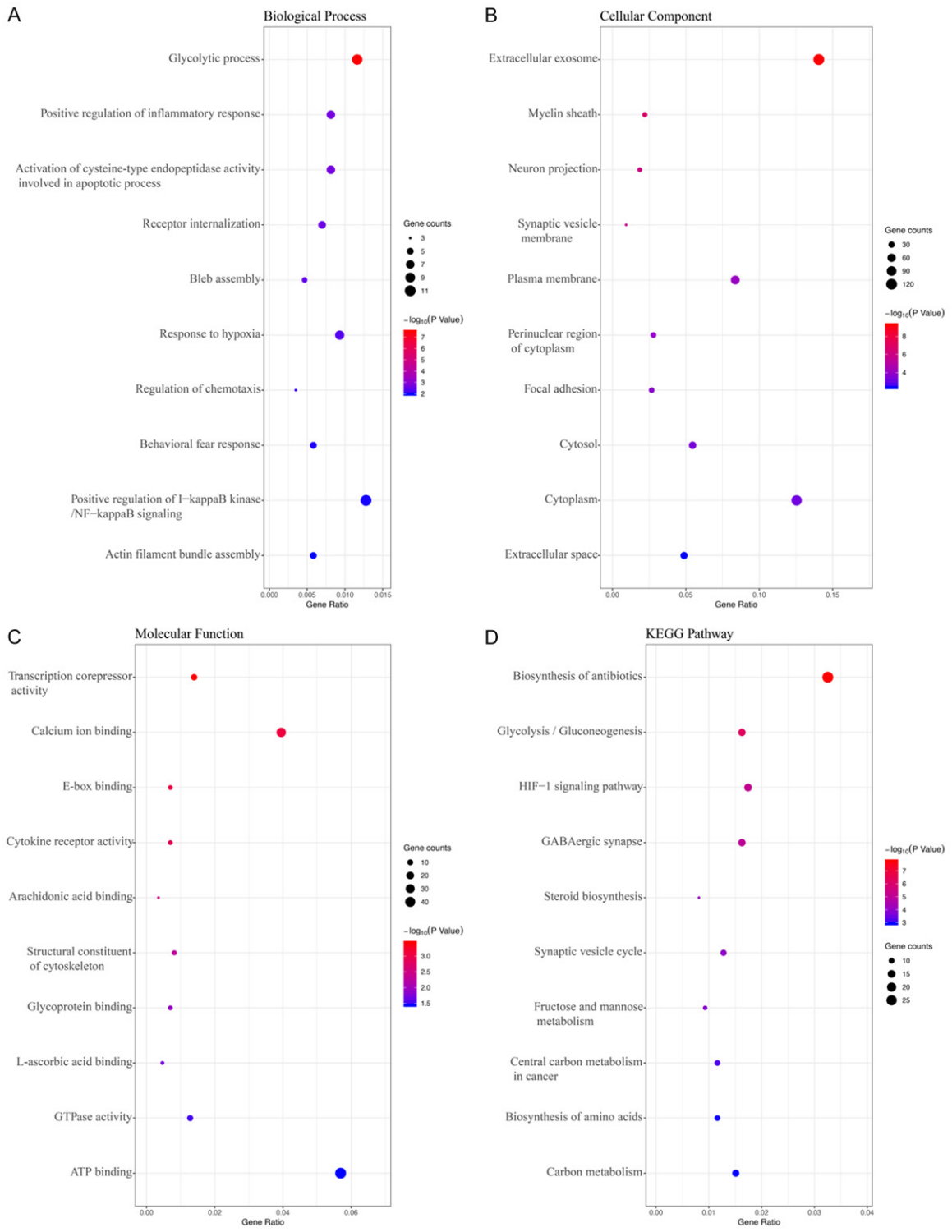


**Figure 9.** GO functions and KEGG pathways for PFKP and STXBP1 and their coexpressed genes. A. Enriched biological processes. B. Enriched cellular components. C. Enriched molecular functions. D. Enriched KEGG pathways.

of small populations of medulloblastoma patients have demonstrated the significance of single biological prognostic markers, such as MYC amplifications, chromosome 17p deletions, the apoptotic index, TrkC expression, the Ki-67 index, and chromosome 6q status [7, 13,

29-33]. In conclusion, single clinical, histopathological and molecular features have only limited prognostic significance.

The lack of effective and reliable prognostic biomarkers or models remains a major problem for improving the prognosis of medulloblastoma patients. Recent large-scale genomic analyses have enabled further characterization of medulloblastoma in ways that have both prognostic and therapeutic significance. In contrast to previous studies that focused more on expression of a single mRNA or microRNA [7, 8, 10, 13, 29-33], our study is the first to develop a multigene-based risk score model to predict the prognosis of medulloblastoma patients. Survival analysis also indicated that our two-gene model can serve as an independent prognostic factor for medulloblastoma, with good accuracy and stability compared with other clinicopathological parameters. Moreover, the comprehensive prognostic model, composed of the two-gene signature integrated with clinicopathological characteristics, exhibited a more favorable predictive ability (C-index 0.823) with regard to clinical outcome for both 3-year and 5-year OS rates of medulloblastoma patients compared with the isolated two-gene prognostic risk score model (C-index 0.752). To date, however, only a few studies have attempted to integrate multiple clinical and biological markers to predict clinical outcomes for medulloblastoma patients. Gajjar et al. [34], Ray et al. [27] and Pietsch et al. [7] all treated every single gene pattern as an independent molecular feature in univariate and multivariate analyses to construct prognostic models [7, 27, 34]. In contrast, our study utilized multiple prognosis-associated genes to establish an isolated risk score model, which was then treated as the molecular feature, combining this with other clinicopathological variables to independently predict the OS of medulloblastoma patients. To our knowledge, this is the first study in which a multigene-based risk score model is used to predict the prognosis of medulloblastoma patients.

Platelet isoform of phosphofructokinase (PFKP) and syntaxin-binding protein 1 (STXBP1) were determined to be the most significant prognosis-related genes in our risk score model. Both were found to be significantly underexpressed in medulloblastoma tissues, with low expression of PFKP predicting a better OS but low expression of STXBP1 predicting a poorer OS. The PFKP gene encodes an enzyme that has a key role in glycolysis regulation [35] and may be involved in metabolic reprogramming in several cancers, including cancers of the brain, bladder, kidney, and lung [36-40]. Previous studies have demonstrated that PFKP is a crucial player in many steps of cancer initiation and metastasis [35]. Sanzey et al. [36] reported that PFKP silencing resulted in a prominent increase in survival in mice. As a result, phosphofructokinase 1 (PFK1), encoded by the PFKP gene, is regarded as an important therapeutic target to address the metabolic escape mechanisms of glioblastoma. However, the roles of PFKP in medulloblastoma have not been previously studied. The STXBP1 gene encodes a syntaxin-binding protein that appears to play a role in the release of neurotransmitters via the regulation of syntaxin, a transmembrane attachment protein receptor. Few studies have investigated the roles of STXBP1 in brain tumors. Because it is expressed in postmitotic neurons of the adult human brain and in tumors of neuronal origin, STXBP1 may serve as a molecular tool to understand the growth and differentiation of the nervous system in general [41]. Lou et al. [42] identified STXBP1 as the most significantly downregulated hub gene, which may promote the progression of glioblastoma. In summary, the roles of PFKP and STXBP1 in medulloblastoma have not been reported and remain obscure. Our study provides evidence that PFKP may act as a promoter and STXBP1 as a suppressor in medulloblastoma, which should be investigated by further studies.

There are some limitations to the present study. Due to the limited clinical and molecular information of our cohort, we could not compare the prognostic value of our two-gene signature with molecular subgroups, including WNT, SHH, group 3, and group 4. Finally, the roles of PFKP and STXBP1 in medulloblastoma have not been reported in the literature, and future studies on the underlying mechanisms of these two genes in the development and progression of medulloblastoma are warranted.

In conclusion, by performing a comprehensive gene expression profile assessment, we identified a two-gene risk score model that significantly predicted the prognosis of medulloblas-

toma patients. This two-gene risk score model is a promising independent prognostic factor for medulloblastoma. Furthermore, the comprehensive prognostic model, composed of the two-gene signature integrated with clinicopathological features, exhibited favorable prognostic value for medulloblastoma patients. Further studies with large-sized, multicenter and prospective clinical cohorts are needed to verify the prognostic model developed in this study.

## Acknowledgements

Dr. Wang is grateful for the invaluable support received from his parents and, in particular, Prof. Bing Xing over the years. This study was supported by the Graduate Innovation Fund of the Chinese Academy of Medical Sciences and Peking Union Medical College (2019-1002-73).

Informed consent was obtained from all individual participants included in the study.

## Disclosure of conflict of interest

None.

**Address correspondence to:** Dr. Bing Xing, Department of Neurosurgery, Peking Union Medical College Hospital, Chinese Academy of Medical Sciences and Peking Union Medical College, No. 1 Shuaifuyuan, Dongcheng District, Beijing 100730, P. R. China. E-mail: xingbingemail@aliyun.com

## References

[1] Millard NE and De Braganca KC. Medulloblastoma. J Child Neurol 2016; 31: 1341-1353.

[2] Ramaswamy V and Taylor MD. Medulloblastoma: from myth to molecular. J Clin Oncol 2017; 35: 2355-2363.

[3] Ostrom QT, Gittleman H, Truitt G, Boscia A, Kruchko C and Barnholtz-Sloan JS. CBTRUS statistical report: primary brain and other central nervous system tumors diagnosed in the United States in 2011-2015. Neuro Oncol 2018; 20: iv1-iv86.

[4] Khatua S, Song A, Sridhar DC and Mack SC. Childhood medulloblastoma: current therapies, emerging molecular landscape and newer therapeutic insights. Curr Neuropharmacol 2018; 16: 1045-1058.

[5] Ramaswamy V, Remke M, Adamski J, Bartels U, Tabori U, Wang X, Huang A, Hawkins C, Mabbott D, Laperriere N, Taylor MD and Bouffet E. Medulloblastoma subgroup-specific outcomes in irradiated children: who are the true high-risk patients? Neuro Oncol 2016; 18: 291-297.

[6] Zeltzer PM, Boyett JM, Finlay JL, Albright AL, Rorke LB, Milstein JM, Allen JC, Stevens KR, Stanley P, Li H, Wisoff JH, Geyer JR, McGuire-Cullen P, Stehbens JA, Shurin SB and Packer RJ. Metastasis stage, adjuvant treatment, and residual tumor are prognostic factors for medulloblastoma in children: conclusions from the children's cancer group 921 randomized phase III study. J Clin Oncol 1999; 17: 832-845.

[7] Pietsch T, Schmidt R, Remke M, Korshunov A, Hovestadt V, Jones DT, Felsberg J, Kaulich K, Goschzik T, Kool M, Northcott PA, von Hoff K, von Bueren AO, Friedrich C, Mynarek M, Skladny H, Fleischhack G, Taylor MD, Cremer F, Lichter P, Faldum A, Reifenberger G, Rutkowski S and Pfister SM. Prognostic significance of clinical, histopathological, and molecular characteristics of medulloblastomas in the prospective HIT2000 multicenter clinical trial cohort. Acta Neuropathol 2014; 128: 137-149.

[8] Northcott PA, Korshunov A, Witt H, Hielscher T, Eberhart CG, Mack S, Bouffet E, Clifford SC, Hawkins CE, French P, Rutka JT, Pfister S and Taylor MD. Medulloblastoma comprises four distinct molecular variants. J Clin Oncol 2011; 29: 1408-1414.

[9] Louis DN, Perry A, Reifenberger G, von Deimling A, Figarella-Branger D, Cavenee WK, Ohgaki H, Wiestler OD, Kleihues P and Ellison DW. The 2016 World Health Organization classification of tumors of the central nervous system: a summary. Acta Neuropathol 2016; 131: 803-820.

[10] Ramaswamy V, Remke M, Bouffet E, Bailey S, Clifford SC, Doz F, Kool M, Dufour C, Vassal G, Milde T, Witt O, von Hoff K, Pietsch T, Northcott PA, Gajjar A, Robinson GW, Padovani L, Andre N, Massimino M, Pizer B, Packer R, Rutkowski S, Pfister SM, Taylor MD and Pomeroy SL. Risk stratification of childhood medulloblastoma in the molecular era: the current consensus. Acta Neuropathol 2016; 131: 821-831.

[11] Gibson P, Tong Y, Robinson G, Thompson MC, Currle DS, Eden C, Kranenburg TA, Hogg T, Poppleton H, Martin J, Finkelstein D, Pounds S, Weiss A, Patay Z, Scoggins M, Ogg R, Pei Y, Yang ZJ, Brun S, Lee Y, Zindy F, Lindsey JC, Taketo MM, Boop FA, Sanford RA, Gajjar A, Clifford SC, Roussel MF, McKinnon PJ, Gutmann DH, Ellison DW, Wechsler-Reya R and Gilbertson RJ. Subtypes of medulloblastoma have distinct developmental origins. Nature 2010; 468: 1095-1099.

[12] Edgar R, Domrachev M and Lash AE. Gene expression omnibus: NCBI gene expression and hybridization array data repository. Nucleic Acids Res 2002; 30: 207-210.

[13] Pomeroy SL, Tamayo P, Gaasenbeek M, Sturla LM, Angelo M, McLaughlin ME, Kim JY, Goum-

nerova LC, Black PM, Lau C, Allen JC, Zagzag D, Olson JM, Curran T, Wetmore C, Biegel JA, Poggio T, Mukherjee S, Rifkin R, Califano A, Stolovitzky G, Louis DN, Mesirov JP, Lander ES and Golub TR. Prediction of central nervous system embryonal tumour outcome based on gene expression. Nature 2002; 415: 436-442.

[14] Robinson MD, McCarthy DJ and Smyth GK. edgeR: a Bioconductor package for differential expression analysis of digital gene expression data. Bioinformatics 2010; 26: 139-140.

[15] Wang Z, Gao L, Guo X, Feng C, Deng K, Lian W and Xing B. Identification of microRNAs associated with the aggressiveness of prolactin pituitary tumors using bioinformatic analysis. Oncol Rep 2019; 42: 533-548.

[16] Wang L, Cao C, Ma Q, Zeng Q, Wang H, Cheng Z, Zhu G, Qi J, Ma H, Nian H and Wang Y. RNA-seq analyses of multiple meristems of soybean: novel and alternative transcripts, evolutionary and functional implications. BMC Plant Biol 2014; 14: 169.

[17] Linden A and Yarnold PR. Modeling time-to-event (survival) data using classification tree analysis. J Eval Clin Pract 2017; 23: 1299-1308.

[18] Nagashima K and Sato Y. Information criteria for Firth's penalized partial likelihood approach in Cox regression models. Stat Med 2017; 36: 3422-3436.

[19] Zeng JH, Liang L, He RQ, Tang RX, Cai XY, Chen JQ, Luo DZ and Chen G. Comprehensive investigation of a novel differentially expressed lncRNA expression profile signature to assess the survival of patients with colorectal adenocarcinoma. Oncotarget 2017; 8: 16811-16828.

[20] Chen H, Kong Y, Yao Q, Zhang X, Fu Y, Li J, Liu C and Wang Z. Three hypomethylated genes were associated with poor overall survival in pancreatic cancer patients. Aging (Albany NY) 2019; 11: 885-897.

[21] Harrell FE, Lee KL and Mark DB. Multivariable prognostic models: issues in developing models, evaluating assumptions and adequacy, and measuring and reducing errors. Stat Med 1996; 15: 361-387.

[22] Alba AC, Agoritsas T, Walsh M, Hanna S, Iorio A, Devereaux PJ, McGinn T and Guyatt G. Discrimination and calibration of clinical prediction models: users' guides to the medical literature. JAMA 2017; 318: 1377-1384.

[23] Yang S, Kim CY, Hwang S, Kim E, Kim H, Shim H and Lee I. COEXPEDIA: exploring biomedical hypotheses via co-expressions associated with medical subject headings (MeSH). Nucleic Acids Res 2017; 45: D389-D396.

[24] Huang DW, Sherman BT and Lempicki RA. Systematic and integrative analysis of large gene lists using DAVID bioinformatics resources. Nat Protoc 2009; 4: 44-57.

[25] Ashburner M, Ball CA, Blake JA, Botstein D, Butler H, Cherry JM, Davis AP, Dolinski K, Dwight SS, Eppig JT, Harris MA, Hill DP, Issel-Tarver L, Kasarskis A, Lewis S, Matese JC, Richardson JE, Ringwald M, Rubin GM and Sherlock G. Gene ontology: tool for the unification of biology. The gene ontology consortium. Nat Genet 2000; 25: 25-29.

[26] Kanehisa M, Furumichi M, Tanabe M, Sato Y and Morishima K. KEGG: new perspectives on genomes, pathways, diseases and drugs. Nucleic Acids Res 2017; 45: D353-D361.

[27] Ray A, Ho M, Ma J, Parkes RK, Mainprize TG, Ueda S, McLaughlin J, Bouffet E, Rutka JT and Hawkins CE. A clinicobiological model predicting survival in medulloblastoma. Clin Cancer Res 2004; 10: 7613-7620.

[28] Rutkowski S, Gerber NU, von Hoff K, Gnekow A, Bode U, Graf N, Berthold F, Henze G, Wolff JE, Warmuth-Metz M, Soerensen N, Emser A, Ottensmeier H, Deinlein F, Schlegel PG, Kortmann RD, Pietsch T and Kuehl J. Treatment of early childhood medulloblastoma by postoperative chemotherapy and deferred radiotherapy. Neuro Oncol 2009; 11: 201-210.

[29] Bigner SH, Friedman HS, Vogelstein B, Oakes WJ and Bigner DD. Amplification of the c-myc gene in human medulloblastoma cell lines and xenografts. Cancer Res 1990; 50: 2347-2350.

[30] Badiali M, Pession A, Basso G, Andreini L, Rigobello L, Galassi E and Giangaspero F. N-myc and c-myc oncogenes amplification in medulloblastomas. Evidence of particularly aggressive behavior of a tumor with c-myc amplification. Tumori 1991; 77: 118-121.

[31] Batra SK, McLendon RE, Koo JS, Castelino-Prabhu S, Fuchs HE, Krischer JP, Friedman HS, Bigner DD and Bigner SH. Prognostic implications of chromosome 17p deletions in human medulloblastomas. J Neurooncol 1995; 24: 39-45.

[32] Bruggers CS, Tai KF, Murdock T, Sivak L, Le K, Perkins SL, Coffin CM and Carroll WL. Expression of the c-Myc protein in childhood medulloblastoma. J Pediatr Hematol Oncol 1998; 20: 18-25.

[33] Korshunov A, Savostikova M and Ozerov S. Immunohistochemical markers for prognosis of average-risk pediatric medulloblastomas. The effect of apoptotic index, TrkC, and c-myc expression. J Neurooncol 2002; 58: 271-279.

[34] Gajjar A, Hernan R, Kocak M, Fuller C, Lee Y, McKinnon PJ, Wallace D, Lau C, Chintagumpala M, Ashley DM, Kellie SJ, Kun L and Gilbertson RJ. Clinical, histopathologic, and molecular markers of prognosis: toward a new disease risk stratification system for medulloblastoma. J Clin Oncol 2004; 22: 984-993.

[35] Lang L, Chemmalakuzhy R, Shay C and Teng Y. PFKP signaling at a glance: an emerging me-

diator of cancer cell metabolism. Adv Exp Med Biol 2019; 1134: 243-258.
[36] Sanzey M, Rahim SAA, Oudin A, Dirkse A, Kaoma T, Vallar L, Herold-Mende C, Bjerkvig R, Golebiewska A and Niclou SP. Comprehensive analysis of glycolytic enzymes as therapeutic targets in the treatment of glioblastoma. PLoS One 2015; 10: e0123544.
[37] Wang Y, Mei Q, Ai YQ, Li RQ, Chang L, Li YF, Xia YX, Li WH and Chen Y. Identification of lung cancer oncogenes based on the mRNA expression and single nucleotide polymorphism profile data. Neoplasma 2015; 62: 966-973.
[38] Wang J, Zhang P, Zhong J, Tan M, Ge J, Tao L, Li Y, Zhu Y, Wu L, Qiu J and Tong X. The platelet isoform of phosphofructokinase contributes to metabolic reprogramming and maintains cell proliferation in clear cell renal cell carcinoma. Oncotarget 2016; 7: 27142-27157.
[39] Agostini M, Romeo F, Inoue S, Niklison-Chirou MV, Elia AJ, Dinsdale D, Morone N, Knight RA, Mak TW and Melino G. Metabolic reprogramming during neuronal differentiation. Cell Death Differ 2016; 23: 1502-1514.
[40] Sun CM, Xiong DB, Yan Y, Geng J, Liu M and Yao XD. Genetic alteration in phosphofructokinase family promotes growth of muscle-invasive bladder cancer. Int J Biol Markers 2016; 31: e286-e293.
[41] Kalidas S, Santosh V, Shareef MM, Shankar SK, Christopher R and Shetty KT. Expression of p67 (Munc-18) in adult human brain and neuroectodermal tumors of human central nervous system. Acta Neuropathol 2000; 99: 191-198.
[42] Lou W, Ding B, Xu L and Fan W. Construction of potential glioblastoma multiforme-related miRNA-mRNA regulatory network. Front Mol Neurosci 2019; 12: 66.

**Supplementary Table 1.** Primers for real-time PCR

| Genes | Forward (5' to 3') | Reverse (5' to 3') |
|---|---|---|
| PFKP | TGGGAGTGGAGGCAGTCAT | GTCGCTTGTAGGTGTTCAGGT |
| STXBP1 | GGGTATGGAACGGTAGAAA | GTAGGGACTGGAATGAAGATAG |
| GAPDH | TGACTTCAACAGCGACACCCA | CACCCTGTTGCTGTAGCCAAA |

**Supplementary Table 2.** The differentially expressed genes between medulloblastoma and normal cerebellum samples

| Gene | logFC | AveExpr | t | *P*. Value | adj.P.Val | B |
|---|---|---|---|---|---|---|
| Upregulated | | | | | | |
| EEF1A1 | 2.538481 | 12.672487 | 4.28201 | 5.3612E-05 | 0.00415432 | 1.66804231 |
| COL1A1 | 2.378493 | 12.003382 | 3.584391 | 0.00059496 | 0.02441355 | -0.5639775 |
| TMSB10 | 2.329815 | 11.667048 | 5.04582 | 3.0073E-06 | 0.00044665 | 4.37323578 |
| CD24 | 2.03645 | 8.797425 | 3.863177 | 0.0002341 | 0.01376097 | 0.29684805 |
| VIM | 1.999864 | 11.913215 | 3.574618 | 0.00061427 | 0.02488161 | -0.5933478 |
| ACTB | 1.967914 | 13.010389 | 5.015034 | 3.3918E-06 | 0.00049347 | 4.25978276 |
| SOX4 | 1.925101 | 11.605467 | 3.896045 | 0.00020916 | 0.01274467 | 0.40118173 |
| FN1 | 1.85657 | 9.870389 | 3.265095 | 0.00164363 | 0.0461265 | -1.4934931 |
| GNB1 | 1.807946 | 10.9553 | 5.697208 | 2.203E-07 | 4.7591E-05 | 6.84489322 |
| SMARCA4 | 1.787274 | 9.303171 | 4.216695 | 6.783E-05 | 0.0050371 | 1.44846332 |
| RPL29 | 1.759057 | 12.057696 | 3.548295 | 0.0006693 | 0.02615332 | -0.6721683 |
| RPLP0 | 1.72707 | 13.787328 | 3.720766 | 0.00037891 | 0.01822842 | -0.1483705 |
| CCND2 | 1.681113 | 11.443201 | 3.519371 | 0.00073515 | 0.02715468 | -0.7583039 |
| YBX1 | 1.49619 | 11.553288 | 6.505679 | 7.435E-09 | 2.779E-06 | 10.0612907 |
| PABPC1 | 1.466484 | 12.048551 | 3.287016 | 0.00153574 | 0.04414645 | -1.4317109 |
| MDK | 1.408007 | 11.805854 | 3.591316 | 0.00058162 | 0.02427796 | -0.5431355 |
| TUBB | 1.366906 | 14.082475 | 4.550575 | 1.9986E-05 | 0.00222631 | 2.59156652 |
| CCNG1 | 1.317474 | 8.27372 | 3.727938 | 0.00036992 | 0.01821324 | -0.1262166 |
| HMGB2 | 1.314427 | 8.453733 | 3.835566 | 0.00025721 | 0.01432558 | 0.20965794 |
| PCBP2 | 1.267703 | 12.191399 | 3.483105 | 0.00082639 | 0.02945661 | -0.8655939 |
| ITGB1 | 1.255156 | 9.997868 | 3.590937 | 0.00058234 | 0.02427796 | -0.5442748 |
| TOP2A | 1.254234 | 9.250008 | 4.30657 | 4.9049E-05 | 0.00384252 | 1.7511347 |
| FSCN1 | 1.25236 | 12.760222 | 3.696992 | 0.00041021 | 0.01886699 | -0.2215919 |
| RPN2 | 1.242964 | 9.993432 | 3.355394 | 0.00124039 | 0.03844661 | -1.2370251 |
| PRMT1 | 1.24098 | 11.664696 | 3.946271 | 0.00017591 | 0.01119723 | 0.56172713 |
| HMGN2 | 1.231314 | 11.042082 | 3.262718 | 0.00165575 | 0.0461265 | -1.5001744 |
| TCF3 | 1.218019 | 9.149746 | 3.639458 | 0.00049646 | 0.02190689 | -0.3974537 |
| SMARCA4 | 1.201879 | 10.456384 | 4.935102 | 4.6284E-06 | 0.00063938 | 3.96680051 |
| RPLP1 | 1.167442 | 13.248213 | 3.321113 | 0.00138105 | 0.04136767 | -1.3349977 |
| ODC1 | 1.161828 | 11.61622 | 3.522837 | 0.00072694 | 0.02699156 | -0.7480085 |
| MAZ | 1.132894 | 9.719497 | 3.928743 | 0.0001869 | 0.01166702 | 0.50554813 |
| CBX3 | 1.127179 | 7.766966 | 3.611856 | 0.00054372 | 0.02335033 | -0.481145 |
| COL6A2 | 1.113687 | 10.435635 | 3.565164 | 0.00063352 | 0.02524987 | -0.6217045 |
| PPIB | 1.068116 | 10.758278 | 3.698937 | 0.00040756 | 0.01886676 | -0.2156114 |
| EIF4B | 1.062685 | 10.529136 | 3.332689 | 0.00133196 | 0.04040642 | -1.3019987 |
| IMPDH2 | 1.025355 | 10.521864 | 3.305679 | 0.00144916 | 0.04252449 | -1.3788653 |
| PDIA3 | 1.006196 | 9.02399 | 3.838472 | 0.00025468 | 0.01432558 | 0.21881378 |
| Downregulated | | | | | | |
| KCTD2 | -1.004962 | 10.218443 | -3.964435 | 0.00016519 | 0.01070561 | 0.62011741 |

| | | | | | | |
|---|---|---|---|---|---|---|
| TMEM151B | -1.011556 | 9.077583 | -4.886442 | 5.5865E-06 | 0.00072997 | 3.78958685 |
| ATP5O | -1.017491 | 8.815119 | -3.429117 | 0.00098227 | 0.03320526 | -1.0238355 |
| GABRA1 | -1.027386 | 8.237936 | -5.542195 | 4.1487E-07 | 8.4502E-05 | 6.24535297 |
| SLC1A6 | -1.056038 | 9.817112 | -4.829401 | 6.9575E-06 | 0.00088572 | 3.58297923 |
| PTK2B | -1.057713 | 8.346553 | -6.238417 | 2.3122E-08 | 6.3397E-06 | 8.98351718 |
| BCL6 | -1.057734 | 7.676724 | -4.437528 | 3.039E-05 | 0.00281362 | 2.19888982 |
| PFKP | -1.086018 | 8.569962 | -4.342424 | 4.3055E-05 | 0.00352807 | 1.8729418 |
| FGF9 | -1.0869 | 8.630849 | -4.474997 | 2.6464E-05 | 0.00258444 | 2.32842135 |
| PPP3CA | -1.087309 | 8.326598 | -5.192059 | 1.691E-06 | 0.00028349 | 4.91661788 |
| RUNX1T1 | -1.095114 | 8.563353 | -4.237981 | 6.2838E-05 | 0.00471546 | 1.51979971 |
| DPP6 | -1.122927 | 8.852233 | -3.935803 | 0.0001824 | 0.01150705 | 0.52815851 |
| NAP1L3 | -1.14382 | 7.41058 | -3.539467 | 0.00068878 | 0.02629464 | -0.6985122 |
| GOT1 | -1.153486 | 8.772709 | -3.701851 | 0.00040362 | 0.01886676 | -0.2066506 |
| INPP5A | -1.174916 | 8.526295 | -5.961687 | 7.3802E-08 | 1.9486E-05 | 7.88184356 |
| MGLL | -1.191022 | 10.573987 | -3.392968 | 0.00110175 | 0.03570174 | -1.1287898 |
| DNM1 | -1.215033 | 11.035099 | -5.421891 | 6.7502E-07 | 0.00013006 | 5.78465144 |
| KCNK1 | -1.242021 | 6.611438 | -5.216047 | 1.5376E-06 | 0.00026735 | 5.00643722 |
| STXBP1 | -1.243376 | 10.642568 | -3.298294 | 0.00148286 | 0.04294489 | -1.3998033 |
| GABRA6 | -1.264288 | 6.859061 | -6.251127 | 2.1913E-08 | 6.2488E-06 | 9.03448401 |
| TUBB4A | -1.270348 | 9.613768 | -5.459876 | 5.791E-07 | 0.00011468 | 5.92966131 |
| MT3 | -1.289249 | 10.758994 | -5.355047 | 8.8312E-07 | 0.00016568 | 5.5305045 |
| CBLN1 | -1.291544 | 8.894373 | -3.327724 | 0.00135281 | 0.04069273 | -1.3161635 |
| ATP1A2 | -1.294143 | 6.634868 | -6.410525 | 1.1151E-08 | 3.4564E-06 | 9.67615913 |
| TRIM9 | -1.298185 | 7.04659 | -4.755654 | 9.224E-06 | 0.00111454 | 3.3177187 |
| ENO2 | -1.299399 | 10.266533 | -3.242992 | 0.0017596 | 0.04795062 | -1.555478 |
| SORL1 | -1.304403 | 8.310209 | -6.505874 | 7.4288E-09 | 2.779E-06 | 10.062081 |
| SLC12A5 | -1.338029 | 6.551949 | -5.879824 | 1.0371E-07 | 2.5495E-05 | 7.5591013 |
| GPM6B | -1.376737 | 7.74434 | -3.709532 | 0.00039341 | 0.01867133 | -0.1830096 |
| PCP4 | -1.401126 | 7.927174 | -4.268165 | 5.6362E-05 | 0.00432045 | 1.62133016 |
| CKB | -1.416802 | 9.726276 | -3.235162 | 0.00180249 | 0.04885904 | -1.5773619 |
| TF | -1.423151 | 8.193771 | -4.816363 | 7.3142E-06 | 0.00091479 | 3.53593082 |
| ANK3 | -1.433544 | 7.227315 | -4.440689 | 3.0038E-05 | 0.00281362 | 2.2097937 |
| ATP1B1 | -1.434756 | 8.365901 | -3.985468 | 0.00015355 | 0.01004269 | 0.68794606 |
| CST3 | -1.468756 | 11.777746 | -3.755892 | 0.0003368 | 0.01715033 | -0.0396004 |
| QDPR | -1.481555 | 8.000082 | -6.480651 | 8.2727E-09 | 2.8084E-06 | 9.95985016 |
| PTGDS | -1.552706 | 10.956064 | -3.793857 | 0.00029632 | 0.0159354 | 0.07873201 |
| ALDH1A1 | -1.586181 | 7.265789 | -6.725779 | 2.8957E-09 | 1.3762E-06 | 10.9574668 |
| TSPAN7 | -1.603254 | 9.884463 | -5.132786 | 2.1372E-06 | 0.00033122 | 4.69550275 |
| EFR3A | -1.630272 | 7.094419 | -6.896139 | 1.3893E-09 | 7.0743E-07 | 11.6556495 |
| VSNL1 | -1.665229 | 6.790871 | -6.461932 | 8.9597E-09 | 2.9034E-06 | 9.88404448 |
| ITPR1 | -1.705896 | 6.475495 | -8.470431 | 1.403E-12 | 1.0002E-09 | 18.2095132 |
| SLC1A3 | -1.744028 | 7.70895 | -4.591964 | 1.7121E-05 | 0.00193744 | 2.73671335 |
| PLP1 | -1.751277 | 6.278802 | -7.648055 | 5.2413E-11 | 3.1138E-08 | 14.7712275 |
| PRKCZ | -1.791335 | 7.979327 | -6.49456 | 7.7962E-09 | 2.779E-06 | 10.0162138 |
| PHYHIP | -1.824159 | 9.348432 | -9.732873 | 5.4503E-15 | 9.7139E-12 | 23.4639703 |
| GRM4 | -1.903659 | 9.352769 | -7.844271 | 2.2138E-11 | 1.4347E-08 | 15.5902248 |
| AGT | -1.922606 | 7.624722 | -8.597255 | 8.0197E-13 | 6.3525E-10 | 18.7400337 |
| SPOCK2 | -1.949088 | 10.039431 | -5.062945 | 2.8123E-06 | 0.00042657 | 4.43648935 |
| CRYM | -1.95485 | 8.460849 | -9.758161 | 4.8801E-15 | 9.7139E-12 | 23.5683085 |

| | | | | | | |
|---|---|---|---|---|---|---|
| KIAA0513 | -2.040691 | 9.627983 | -8.751046 | 4.0708E-13 | 4.1458E-10 | 19.3829455 |
| CLU | -2.062903 | 12.180775 | -3.410983 | 0.00104059 | 0.03418614 | -1.0765877 |
| PRUNE2 | -2.107459 | 7.785494 | -6.557309 | 5.9635E-09 | 2.6571E-06 | 10.2708667 |
| SCRN1 | -2.185975 | 9.42464 | -5.804662 | 1.4155E-07 | 3.2552E-05 | 7.26415229 |
| PVALB | -2.286366 | 8.486539 | -11.918852 | 4.6802E-19 | 3.3365E-15 | 32.2513059 |
| ABLIM1 | -2.495643 | 9.391604 | -6.39879 | 1.1722E-08 | 3.4818E-06 | 9.62876733 |
| ALDOC | -2.670672 | 10.498201 | -9.248573 | 4.5543E-14 | 6.4936E-11 | 21.4573386 |
| TIAM1 | -2.752643 | 8.207577 | -8.798265 | 3.3059E-13 | 3.9279E-10 | 19.5802215 |
| SNAP25 | -3.607967 | 8.554881 | -8.693794 | 5.2395E-13 | 4.6691E-10 | 19.1436729 |
| MBP | -3.725658 | 8.516217 | -6.536948 | 6.5057E-09 | 2.7282E-06 | 10.1881681 |

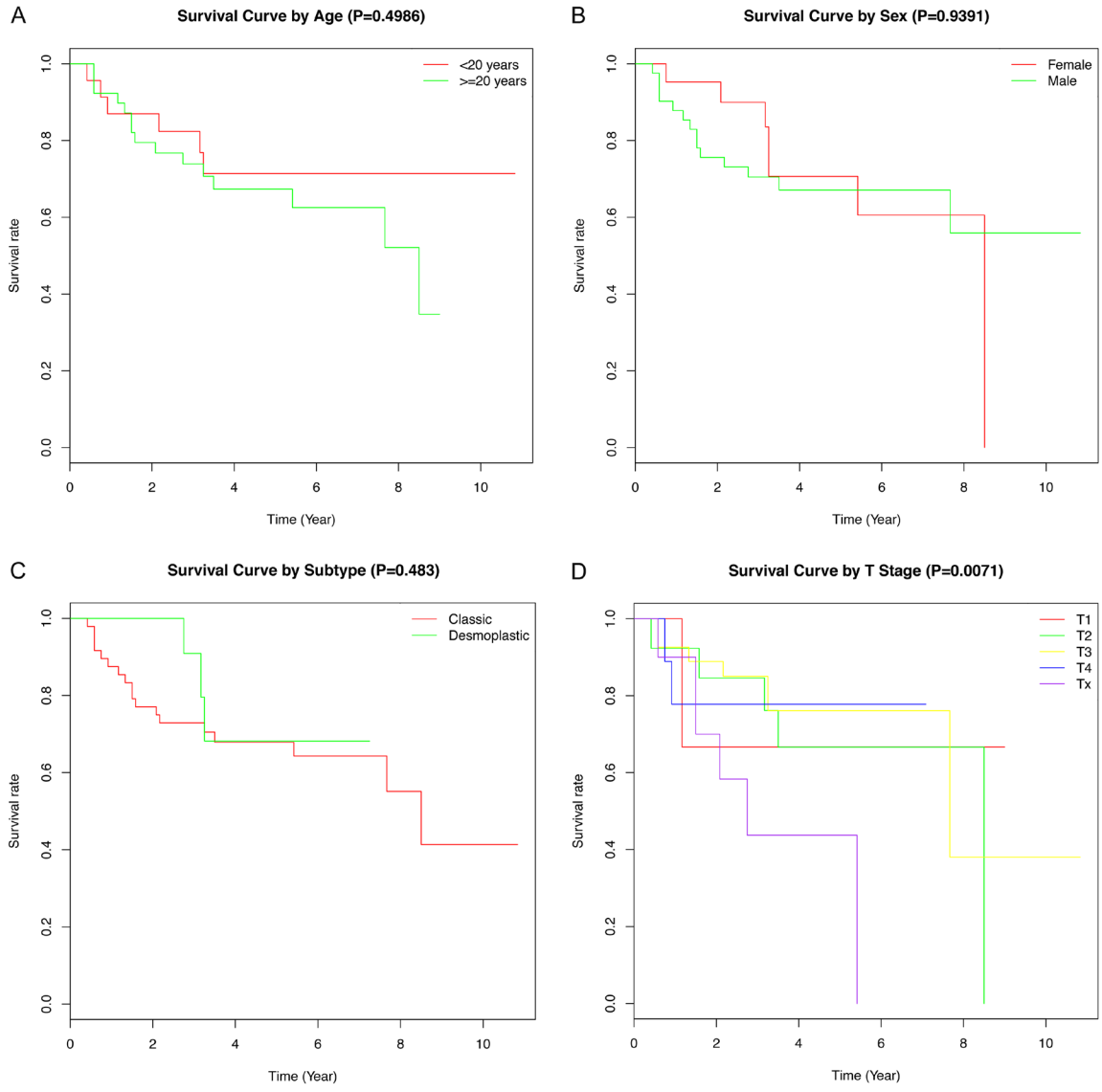

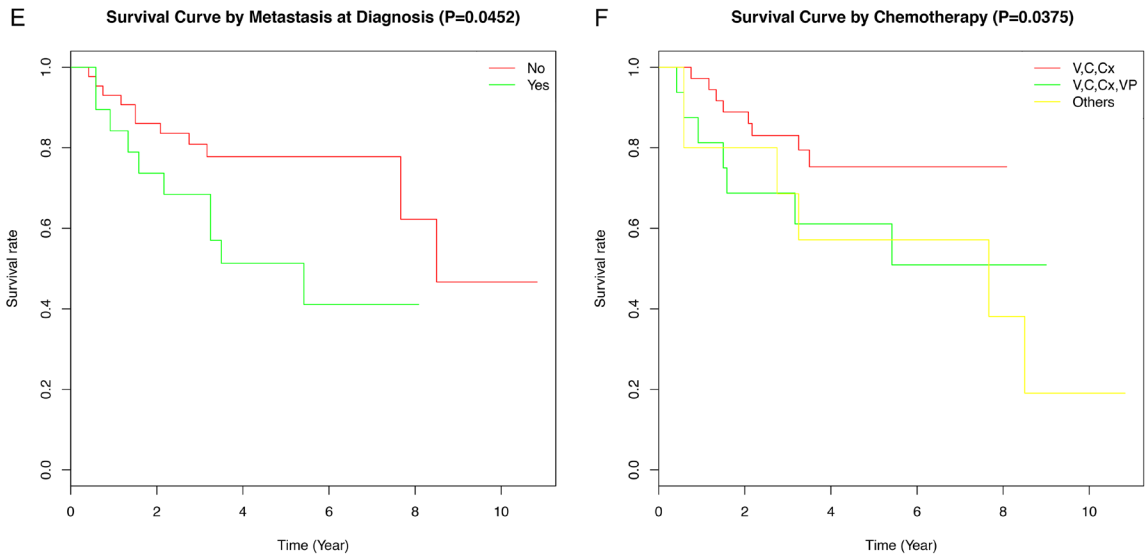


**Supplementary Figure 1.** Kaplan-Meier survival curves and log-rank test for clinicopathologic parameters in 62 medulloblastoma patients.